J Math Chem (2009) 45:460–470
DOI 10.1007/s10910-008-9419-y

ORIGINAL PAPER

Topology and electronic structure of nanotube junctions of tetrapod shape

Kyoko Nakada · Kenji Maeda · Kota Daigoku

Published online: 19 August 2008

Abstract We propose a series of carbon nanostructures in the shape of tetrapod as a kind of three-dimensional junction for carbon nanotubes. The tetrapod junctions are such open networks that are made of sp^2 carbon atoms only, have negative Gaussian curvature, and connect four nanotubes together. We define the structure of standard tetrapod junctions, the simplest one, that have 12 heptagons other than hexagons and have the T_d symmetry.Our tight-binding energy-band calculations for the standard tetrapod junctions of smaller sizes show that their electronic property mainly depends on one particular topological factor: the junctions having a carbon atom in the center of each triangular face of tetrahedron exhibit metallic band structure while the junctions having a benzene ring in the center of the faces are semiconductors. We also find that tetrapod junctions connecting (6,0) nanotubes exhibit a flat band near the Fermi energy in a particular momentum region. The origin of the flat band states can be figured out from the wavefunction distribution. We also show the possibility to extend the standard tetrapod junctions to some non-standard ones that can connect nanotubes of different kinds and/or radii.

Keywords Carbon nanotube · Junction · Topology · Flat band · Energy-band calculation

K. Nakada (✉) · K. Maeda · K. Daigoku
Department of Chemistry and Biological Science, Faculty of Science and Engineering, Aoyama Gakuin University, 5-10-1 Fuchinobe, Sagamihara 229-8558, Japan
e-mail: nakada@chem.aoyama.ac.jp

Present Address:
K. Daigoku
Division of Chemistry, Center for Natural Sciences, College of Liberal Arts and Sciences, Kitasato University, 1-15-1 Kitasato, Sagamihara, Kanagawa, 228-8555, Japan

1 Introduction

One of the most fascinating features of sp^2 carbon materials, such as fullerenes and nanotubes, is the fact that the electronic property is mostly determined by the topology of sp^2 carbon network. The electronic property of nanotubes, for example, to be metallic or semiconducting is determined by a single topological parameter, the chiral vector. The variety of electronic state of fullerenes is also considered to originate from the variety of network topology: different ways of inserting 12 pentagons into a honeycomb network cause different electronic states of fullerene. The network topology is most responsible for the electronic property of sp^2 carbon materials because in these materials the π electrons, whose intrinsic behavior is well described even in the nearest neighbor approximation, govern the electronic state near the Fermi energy. Thanks to this fact, a number of theoretical studies discussing the network topology of carbon materials have always provided useful informations and insight for the electronic property of the materials.

There is no doubt that the junctions connecting multiple nanotubes play a key role in the so-called nanotube electronics that is expected to replace today's silicon-based electronics. Though most of the nanotube junctions, experimentally fabricated at this moment, have rather simple structures such as I, T, Y and X-shapes [1–7], there remain some other structures [8, 9] that have the potential to be a nanotube junction. As such, we study a series of nanotube junctions that have a shape of tetrapod. The nanotube junctions of tetrapod shape connect four nanotubes and form three-dimensional nanotube networks of diamond structure. We study the relation between the electronic property and the topology of the nanotube junctions of tetrapod shape. Though such a junction of exact tetrapod shape has not yet been synthesized or found as a real carbon material, the recently discovered material, carbon nanofoam [10, 11], should have a similar structure in order to realize a multiply branched structure of nanotube. To achieve a simple and clear understanding of the electronic property of nanotube junctions is therefore useful to provide a perspective to the rich variety of sp^2-carbon based materials.

2 Nanotube junctions of tetrapod shape

We define the topological structure of the tetrapod junctions studied in this work in order to focus attention to the relation between the electronic structure and the topology of junctions. There are, apparently, infinite number of junctions that have a tetrapod shape in common but have a variety of topologies. For such tetrapod junctions there already exist the theoretical studies that propose or generate some model structures as three-connected open networks made of sp^2 carbons [8, 9, 12–18]. We, in this work, require two topological conditions to define the simplest tetrapod junctions as a standard, i.e., a prototype, of nanotube junctions of tetrapod shape.

As a premise, we consider the tetrapod junctions as a series of open networks of tetrapod shape made of sp^2 carbon atoms only. The tetrapod junctions are therefore a series of three-connected networks with some negative Gaussian curvatures to make

the tetrapod shape as a whole. As a material, the tetrapod junctions form a hypothetical crystal of pure sp^2 carbon in three dimensions.

The first condition for the tetrapod junctions is the requirement that they contain only heptagons other than hexagons. It is a well established argument that at least one ring larger than hexagon is necessary to make a negative Gaussian curvature in a three-connected network. There are many possible structures that contain octagons, nonagons or other larger rings [19] and are many possible structures that contain 5-, 4-, or 3-membered rings together with some rings larger than hexagon [20]. Though some of them may have less strain energy, we, in this study, exclusively consider the tetrapod junctions containing hexagons and heptagons.

The first condition determines the number of heptagon. Since the genus g for the tetrapod junctions is $g=2$, that is the same as a double torus, it is straightforward to derive $F_7=12$ from the relations below

$$6F_6+7F_7 = 3V \tag{1}$$

$$6F_6+7F_7 = 2E \tag{2}$$

$$V + F_6+F_7-E = 2-2g \tag{3}$$

where V, E, F_6 and F_7 are the numbers of vertex, edge, hexagon and heptagon, respectively. All the tetrapod junctions studied in the this paper have therefore 12 heptagons together with hexagons.

As the second condition we impose the T_d symmetry on the tetrapod junctions. This requirement drastically simplify the structure of the junctions: the symmetry of the tetrapod junctions should be the same as the symmetry of regular tetrahedron. The four nanotubes connected by the junction, that correspond to the four vertices of tetrahedron, should therefore be identical and should be armchair or zigzag tubes because of the threefold rotational symmetry of tetrahedron. The task to find the possible structures for the standard tetrapod junctions is now reduced, as the first step, to distribute 12 heptagons onto the surface of tetrahedron that have four identical vertices, six identical edges and four identical faces. There are two solutions for the distribution of 12 heptagons: three heptagons on each face or two heptagons on each edge. The arrangement of the three (two) heptagons on each face (edge) should also satisfy the T_d symmetry.

After putting the two topological conditions above described, we can classify the tetrapod junctions into the eight groups depicted in Fig. 1. We employ two topological factors to describe the eight groups: the type of nanotube and the center of the face of tetrahedron. As the type of nanotube, there are two possibilities, i.e., the armchair or zigzag tube. The center of the triangular face of tetrahedron should be a carbon atom or a benzene ring. This requirement is also due to the T_d symmetry. Considering the two orientations for each of the central atom and central ring, we can choose one of four possibilities as the center of the face. Since there is no restriction in choosing the two factors, i.e., the type of nanotube and the type of face center, all the standard tetrapod junctions are classified into the eight groups.

The arrangement of 12 heptagons are simultaneously determined for each of the eight groups. In order to see that, we view an armchair (zigzag) nanotube as a parallel

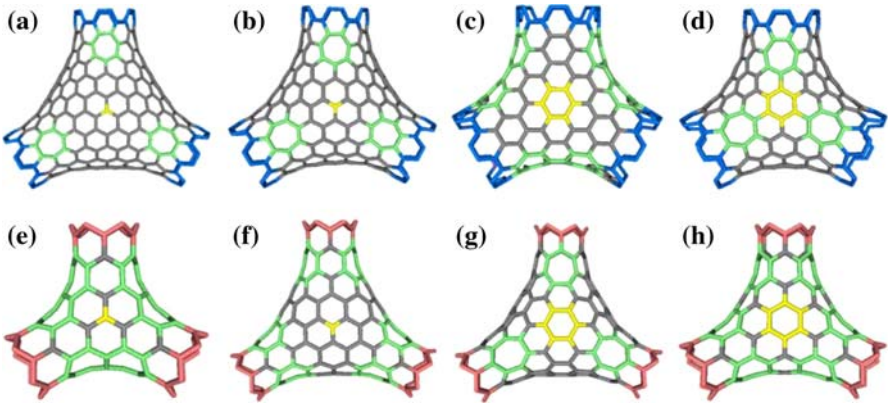

Fig. 1 The standard tetrapod junctions classified into eight groups. The type of nanotube is distincted by the color of blue for armchair and of red for zigzag. The face of tetrahedron, that is a carbon atom (**a**), (**b**), (**e**), (**f**) or a benzene ring (**c**), (**d**), (**g**), (**h**), is marked by yellow. The heptagons distributed on the face (**a**), (**b**), (**d**), (**g**) or on the edge (**c**), (**e**), (**f**), (**h**) are marked by green

alignment of armchair (zigzag) lines that are in a circular shape, that is., the circumference of the tube. Similarly, we consider the area around the face center of a junction as an alignment of armchair or zigzag lines that are parallel to the circumferences of one the four nanotubes. For the junctions in the groups (c) and (g) in Fig. 1, the area around the face center can be seen as an alignment of armchair lines that are parallel to the circumference of one of the four nanotubes or to the horizontal direction in Fig. 1. For the others in Fig. 1, we see an alignment of zigzag lines in the area around the face center. There are two cases: for the junctions in the groups (c), (e), (f) and (h) the alignment of the lines around the face center is the same as the one in the tube, while for the junctions in the groups (a), (b), (d) and (g) the alignment of the lines around the face center is different from the one in the tube. Now we see that the heptagons inserted into the hexagons control the two cases: the heptagons are arranged on the edge of tetrahedron in the former four groups, while the heptagons are arranged on the face of tetrahedron in the latter four groups.

It is worthwhile to remark here the topological line defects that have recently been proposed [21, 22]. The topological line defects are defined as a boundary between the armchair and zigzag lines that are aligned in parallel. As shown in Fig. 2, such a topological line defect can be a sequence of alternating pentagons and heptagons (Fig. 2a), of pentagon–heptagon pairs (Fig. 2b), or of alternating pentagon pairs and octagons (Fig. 2c) in which we can consider the octagons as the merged pentagons and heptagons from the comparison to the line defect in Fig. 2b. We therefore see that heptagons, when they form one of the line defects together with pentagons, can connect the armchair and zigzag lines aligned parallel in two-dimensional sheet or in one-dimensional tube.

A single heptagon in the three-dimensional tetrapod junctions also connects the aligned armchair and zigzag lines. In the tetrapod junctions having three heptagons on each face (Fig. 3a), each heptagon connects the line alignments around the face center and in the tube. The line alignment around the face center is therefore different

from the one in the tube. In the tetrapod junctions having a pair of heptagons on each edge (Fig. 3b), each heptagon again connects the aligned armchair (zigzag) and zigzag (armchair) lines. Nonetheless, the line alignment around the face center is the same as the one in the tube (Fig. 3c), since the heptagons are not placed on the face but on the edge.

We now understand that there is no restriction in choosing the line alignment around the face center and in the tube. By placing three heptagons on each face, we can connect the armchair (zigzag) lines around the face center and the zigzag (armchair) lines in the tube. By placing a pair of heptagons on each edge, in contrast, we can connect the armchair (zigzag) lines around the face center and the armchair (zigzag) lines in the tube. This combination of armchair/zigzag alignments, together with the two possibility for the face center, i.e., a carbon atom or a benzene ring, results in the eight groups shown in Fig. 1.

After selecting one of the eight groups, another three parameters are needed to fully specify the topology of the standard tetrapod junctions: the radius of the armchair/zigzag nanotube, the separation of the three (two) heptagons on the face (edge),

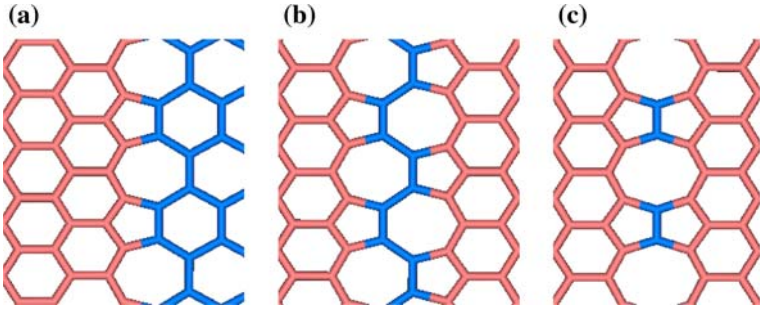

Fig. 2 The topological line defects defined as a boundary between the aligned armchair (in blue) and zigzag (in red) lines. (**a**) The line defect that appears when an alignment of armchair lines is adjacent to an alignment of zigzag lines. (**b**) The line defect that appears when two armchair lines are inserted into an alignment of zigzag lines. (**c**) The line defect that appears when a single armchair line is inserted into an alignment of zigzag lines

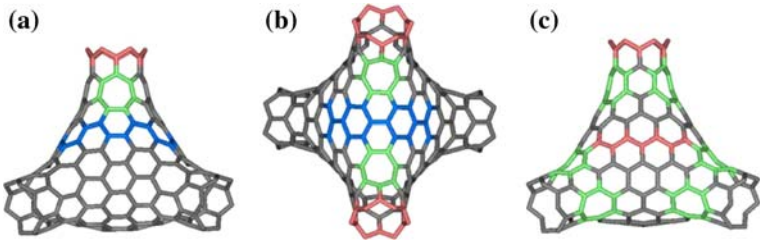

Fig. 3 The role of a single heptagon in a tetrapod junctions. (**a**) The heptagon arranged on the face of tetrahedron connects the aligned armchair and zigzag lines. In the tetrapod junctions with heptagons arranged on the face, the alignment of lines around the face center is therefore different from the one in the tube. (**b**) The heptagon arranged on the edge of tetrahedron also connects the aligned armchair and zigzag lines. The drawing is made for the junction in Fig. 1f. (**c**) The same junction as in (**b**) from another view. The alignment of lines around the face center is the same as the one in the tube

and the length of the nanotube. We took, in this study, the shortest possible nanotube, the shortest possible separation for the three (two) heptagons on the face (edge), and the three thinner nanotubes, i.e., (6,0), (6,6) and (12,0) nanotubes.

3 Electronic structure of tetrapod junctions

For the standard tetrapod junctions of smaller sizes that are defined above, we studied the relation between electronic structure and topology by performing electronic band calculation within the tight-binding approximation. All the tetrapod junctions form a diamond crystal lattice in which a pair of junctions in staggered form make a unit cell. It should be noted that we can form various networks other than normal diamond by using various unit cells. We, in this study, focus attention to the network structure of cubic diamond, i.e., the D-type schwarzites tessellated by hexagons and heptagons.

In Fig. 4 we show the two typical electronic band structures for the tetrapod junctions. Within the calculations we performed, we found that the electronic property of the tetrapod junctions depends on one particular topological factor: the junctions with

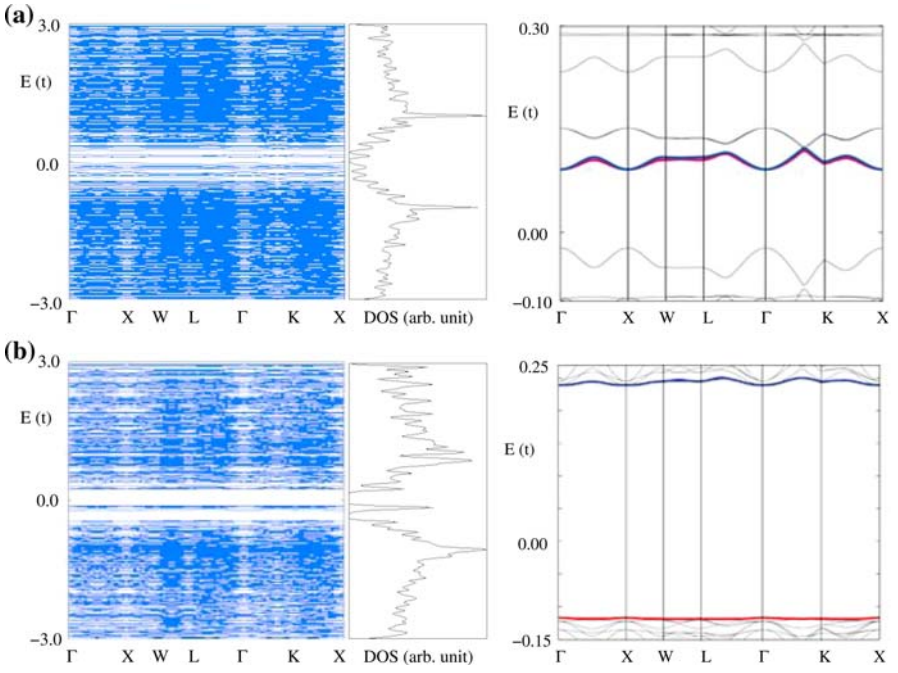

Fig. 4 The electronic band structure and density of states (left) and the magnified band structure near the Fermi energy (right) where the highest occupied and lowest unoccupied bands are indicated by the colors red and blue, respectively. The dispersion relation is drawn along the symmetry points in the first BZ of diamond lattice, and the energy unit is scaled by the transfer integral (t) between the nearest neighbor sites. (**a**) The tetrapod junctions having a carbon atom in the face center show metallic band structure. We show the results for the junction in Fig. 1a as an example. (**b**) The tetrapod junctions having a benzene ring in the face center show semiconducting band structure. The figure is drawn for the junction in Fig. 1c

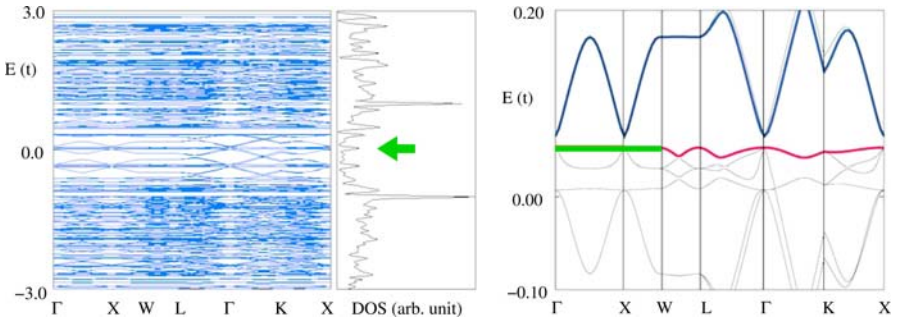

Fig. 5 The electronic structure of the tetrapod junctions connecting (6,0) nanotubes. See the caption in Fig. 4. The partly flat band and the corresponding peak in the density of states are indicated in green. The figure is drawn for the junction in Fig. 1h

a carbon atom at the face center have metallic band structures (Fig. 4a), including the band structures with a very narrow gap, while the junctions with a benzene ring at the face center have semiconducting band structures (Fig. 4b). This tendency holds true for all the standard tetrapod junctions of smaller sizes that we examined. We cannot regard this tendency as a rule. We, however, see from the tendency that the electronic property of nanotube networks connected by the tetrapod junctions does not depend on the nanotube itself but depends on the junction. For example, the three-dimensional nanotube network made of metallic (semiconducting) nanotubes can be semiconducting (metallic) depending on the topology of the tetrapod junction employed in the network. This example suggests the importance to consider the topology of junctions as a part of sp^2 carbon network.

Among the tetrapod junctions we studied, the junctions having (6,0) nanotubes exhibit a partly flat band near the Fermi energy. We show an example in Fig. 5 in that the flat band in a particular momentum region and the corresponding peak in the density of states are emphasized in green. One of the two points to be noted here is the fact that all the tetrapod junctions with (6,0) nanotubes exhibit a flat band regardless of other topological factors. The other point to be noted is the fact that these nanotubes exhibit a flat band in the identical wave number region that corresponds to the boundary lines of the first Brillouin zone (BZ) of the crystal lattice.

With the help of the two facts above described, we can figure out the origin of the flat band states by examining the wavefunction distribution. In Fig. 6a we show the wavefunction distribution of the flat band states at a wave number on the $\Gamma - X$ line in the first BZ. We see that there are nodes of wavefunction at a pair of boundaries of the unit cell and that the direction connecting these boundaries corresponds to the $\Gamma - X$ direction in the wave number space. Now we understand that this node of wavefunction is the origin of the flat band states. The wavefunction, and the corresponding energy, of the whole network cannot vary no matter what the wave number along the $\Gamma - X$ line is, since there is no overlap of the wavefunction component between the adjacent cells in that direction. The same situation is observed along the other two directions that span the first BZ.

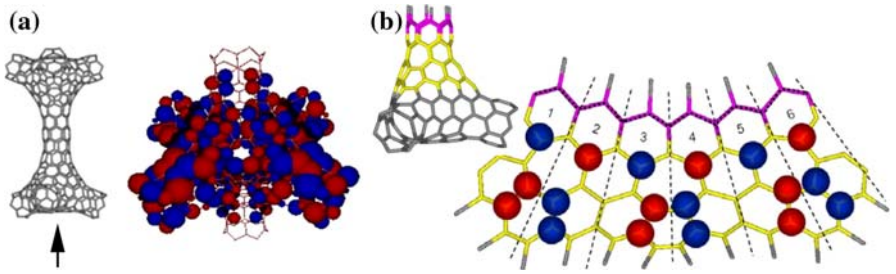

Fig. 6 The wavefunction distribution of the flat band state seen in the tetrapod junctions connecting (6,0) nanotubes. The red/blue coloring and radius of the spheres indicate the phase and amplitude of wavefunction component. (**a**) The skeleton of the unit cell (left) and the wavefunction distribution of the flat band state at a wave number on the $\Gamma - X$ line (right). The figure is drawn for the junction in Fig. 1h, and is drawn from the direction indicated by the arrow. (**b**) Schematic picture of the wavefunction distribution in which the region near one of the (6,0) tubes, the colored region in the inset, are depicted as a projection map. The numbering from 1 to 6 indicates the six hexagons around the circumference of the (6,0) tube. The dotted lines indicate the nodal lines of the wavefunction

The flat band appears in the very vicinity of the Fermi energy for all the tetrapod junctions with (6,0) nanotubes irrespective to other topological factors. In Fig. 6b we show a schematic picture for the wavefunction distribution of Fig. 6a as a projection map that depicts the area near the (6,0) tube. Though the flat band state is not a non-bonding orbital (NBO) of energy zero, the wavefunction distribution near the (6,0) tube is quite similar to an NBO: for each site near the tube, the value of wavefunction components summed up over the three neighboring sites vanishes, while the value does not necessarily vanish for the sites far away from the tube. This similarity to an NBO is the reason that the flat band always appears in the very vicinity of the Fermi energy.

The remaining question about the flat band states is that why it appears in all the tetrapod junctions with (6,0) nanotubes and why it does not appear in the junctions with other nanotubes. The question, in other words, is that why the (6,0) nanotubes do and why other nanotubes do not realize the nodes of wavefunction at the boundaries of the unit cell as shown in Fig. 6a. The clue to answer this question is in the wavefunction distribution near the (6,0) tube. We see in Fig. 6b that there are six nodal lines running along the (6,0) tube and that three of them pass through the heptagons that are adjacent to the six hexagons along the circumference of the tube. It is conceivable that these nodal lines play a crucial role in the flat band states, since all the junctions with (6,0) nanotubes do exhibit the wavefunction distributions that are quite similar to Fig. 6b. Though the flat band state is not an exact NBO, if there are such nodal lines as shown in Fig. 6b, it is expected that the wavefunction components at the boundary of the unit cells, that is emphasized by the color of pink in Fig. 6b, will vanish for sure.

One simple and important fact to be noticed here is that all the tetrapod junctions with (6,0) nanotubes have the topological structure that is identical to the one in Fig. 6b around their (6,0) tubes. No matter what the other topological factors are, the topological structure around the tube is identical to the one in Fig. 6b, if the nanotube in question is a (6,0) tube. Since 12 heptagons are distributed to four nanotubes, three

heptagons for each, if there are only six hexagons around the circumference of tube, no other structure can be possible under the T_d symmetry. We can thus understand that all the tetrapod junctions with (6,0) nanotubes do exhibit the flat band states near the Fermi energy.

The flat band states are not expected to lead to a ferromagnetism in a straightforward way, since the wavefunction distribution is confined within the unit cell. It is, however, worth noting that the flat band states do cause a sharp peak in the density of states in the very vicinity of the Fermi energy. Since the flat band states are realized on each boundary line of the first BZ, higher peak heights in the density of states are expected for the junctions that have the first BZ of smaller area. One possibility is the junctions that connect four (6,0) nanotubes of larger length. Those junctions, however, exhibit a larger number of electronic states that do not contribute to the flat band states. We therefore conclude that the tetrapod junctions with shorter (6,0) nanotubes are the best candidates to exhibit some anomaly in the electronic state near the Fermi energy.

4 Extension to non-standard tetrapod junctions

There are vast possibilities to extend the standard tetrapod junctions to another series of tetrapod junctions of non-standard type. One possibility is the extension to the junctions with chirality. A well-defined and sophisticated method that enables us to generate such chiral junctions is already established: we can systematically generate the structures of chiral tetrapod junctions by applying the map operation of septupling, or Capra, together with some other map operations to the skeleton of tetrahedron [16–18]. Those map operations also enable us to generate the structure of tetrapod junctions with rings other than heptagon.

Here we show another possibility of extension: an extension to the tetrapod junctions that connect nanotubes with different radii. One simple way to connect nanotubes having different radii is to change the relative position of heptagons. Fig. 7 shows an example. By translating the position of the three heptagons that are distributed around one particular nanotube, we can make the junctions that connect three identical nanotubes and one particular nanotube with a different radius. Fig. 8 shows an example of

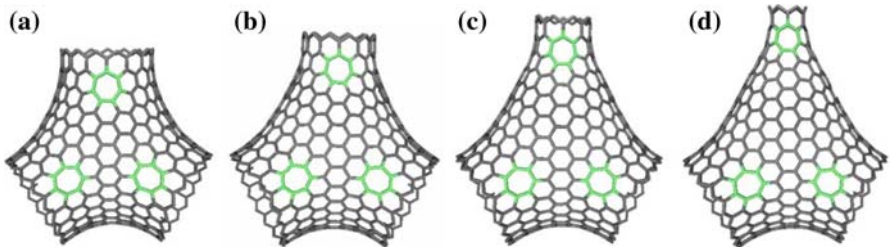

Fig. 7 An example of tetrapod junction that connects nanotubes of two different radii. We can make the radius of one particular nanotube thinner by translating the position of one heptagon that is indicated in green. We depict the junctions that connect three (18,0) tubes and one thinner tube that is a (15,0) tube (**a**), a (12,0) tube (**b**), a (9,0) tube (**c**) and a (6,0) tube (**d**)

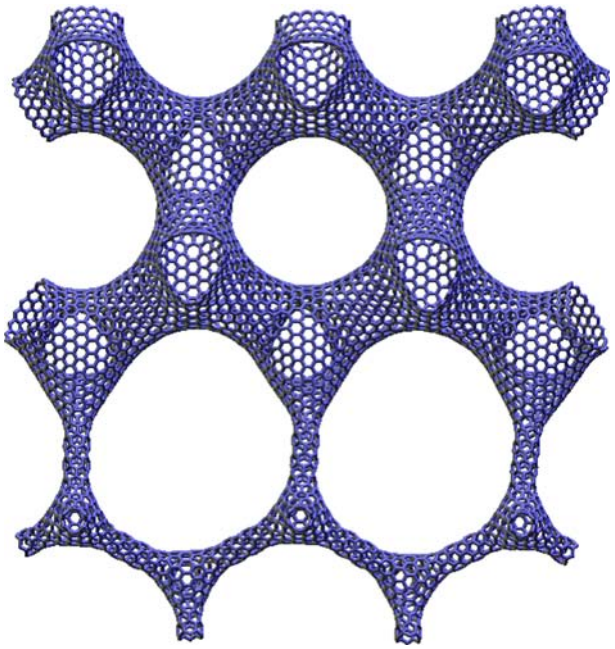

Fig. 8 An example of hypothetical network structures as a porous material that has the pores of two different sizes. A single layer is depicted for simplicity. Along the boundary connecting the upper and lower regions in the figure, the tetrapod junctions in Fig. 7d are used

hypothetical network structures that can be constructed by using the tetrapod junction of such non-standard kind. In addition to the interest in their electronic structure, the three-dimensional networks of this kind rouse our interest in the structure itself. It is expected, for instance, that the nanotube networks of this kind will be useful as a porous material, since they have a well-controlled array of nanopores of different sizes.

5 Conclusion

We have studied the relation between the electronic property and topology of the nanotube junctions of tetrapod shape. Our energy-band calculations within the tight-binding approximation for the standard tetrapod junctions of smaller sizes have showed the possibility that the electronic property of tetrapod junction will be determined mostly by a simple topological factor. We have found that the tetrapod junctions having four nanotubes of a specific kind show a partly flat band near the Fermi level. We have also showed the possibility that extends the standard tetrapod junctions to the junctions of non-standard type.

Acknowledgements The authors gratefully acknowledge Professor Mircea V. Diudea for the fruitful discussions, helpful suggestions and kind invitation to TOPMOL 2006. K. N. is also grateful to Monica Ştefu, Adina Costescu, Csaba L. Nagy, and Simona Cigher for their fruitful discussions and sharing of calculation

programs. Special thanks to Dr. Ibolya Zsoldos are acknowledged for the helpful suggestions and kind sharing of data.

References

1. M. Ouyang, J.-L. Huang, C.L. Cheung, C.M. Lieber, Science **291**, 97 (2001)
2. Z. Yao, H.W.Ch. Postma, L. Balents, C. Dekker, Nature **402**, 273 (1999)
3. D. Zhou, S. Seraphin, Chem. Phys. Lett. **238**, 286 (1995)
4. J. Li, C. Papadopoulos, J. Xu, Nature **402**, 253 (1999)
5. P. Nagy, R. Ehlich, L.P. Biró, J. Gyulai, Appl. Phys. A **70**, 481 (2000)
6. Z. Klusek, S. Datta, P. Byszewski, P. Kowalczyk, W. Kozlowski, Surf. Sci. **507–510**, 577 (2002)
7. Z. Osváth, A.A. Koós, Z.E. Horváth, J. Gyulai, A.M. Benito, M.T. Martínez, W.K. Maser, L.P. Biró, Chem. Phys. Lett. **365**, 338 (2002)
8. I. Zsoldos, Gy. Kakuk, T. Réti, A. Szasz, Model. Simul. Mater. Sci. Eng. **12**, 1 (2004)
9. I. Zsoldos, Gy. Kakuk, J. Janik, L. Pék, Diam. Rel. Mat. **14**, 763 (2005)
10. A.V. Rode, S.T. Hyde, E.G. Gamaly, R.G. Elliman, D.R. McKenzie, S. Bulcock, Appl. Phys. A **69**, S755 (1999)
11. A.V. Rode, E.G. Gamaly, A.G. Christy, J.G. Fitz Gerald, S.T. Hyde, R.G. Elliman, B. Luther-Davies, A.I. Veinger, J. Androulakis, J. Giapintzakis, Phys. Rev. B **70**, 054407 (2004)
12. A.L. Mackay, H. Terrones, Nature **352**, 762 (1991)
13. D. Vanderbilt, J. Tersoff, Phys. Rev. Lett. **68**, 511 (1992)
14. S. Gaito, L. Colombo, G. Benedek, Europhys. Lett. **44**, 525 (1998)
15. N. Park, M. Yoon, S. Berber, J. Ihm, E. Osawa, D. Tománek, Phys. Rev. Lett. **91**, 237204 (2003)
16. M.V. Diudea, Studia Univ. Barbes-Bolyai **48**, 3 (2003)
17. M.V. Diudea, Forma **19**, 131 (2004)
18. M.V. Diudea, J. Chem. Inf. Model. **45**, 1002 (2005)
19. M.V. Diudea, private communication
20. M.V. Diudea, Phys. Chem. Chem. Phys. **7**, 3626 (2005)
21. S. Okada, K. Nakada, K. Kuwabara, K. Daigoku, T. Kawai, Phys. Rev. B **74**, 121412 (2006)
22. K. Nakada, K. Kuwabara, K. Daigoku, T. Kawai, S. Okada, in preparation